Acta Polytechnica CTU Proceedings **45**:59–65, 2023
https://doi.org/10.14311/APP.2023.45.0059

Published by the Czech Technical University in Prague

CONSIDERATIONS ON AN EMBEDDED PILE'S EFFECTIVE LENGTH IN AN ANALYTICAL CALCULATION ACCORDING TO THE COMMENTARY ON THE STN 73 1002 STANDARD

Jakub Stacho*, Monika Súľovská

Slovak University of Technology in Bratislava, Faculty of Civil Engineering, Department of Geotechnics, Radlinského 11, 810 05 Bratislava, Slovakia

* corresponding author: jakub.stacho@stuba.sk

Abstract. The analytical model for calculating the bearing capacity of a pile, presented in the commentary to STN 73 1002 – Pile Foundations, gives a recommendation to reduce the pile's length in the calculation of the shaft resistance. The recommendation is based on Caquot-Kérisel's theory. Especially in the case of embedded piles, reducing a pile's length in the calculation can cause the shaft friction of the embedded pile to be neglected, and the calculated resistance of the pile is thus significantly lower. The results of instrumented static load tests of embedded piles were analysed. The main aim of the study was to verify the validity of reducing the pile's length in the analytical calculation of the shaft resistance. The results of the static load tests analysed did not show any reduction in the shaft friction on the embedded part of the pile. In the form of a parametric study, the effect of reducing the pile's length in the calculation of shaft friction was analysed for different dimensions of embedded piles.

Keywords: Design of pile, effective length of pile, length of pile, resistance of pile, shaft resistance.

1. Introduction

The vertical bearing capacity of the pile can be determined using various analytical calculation models, e.g., [1–3]. The analytical calculation model, which is stated in detail in the commentary on the STN 73 1002 standard [4], is the one most used in Slovakia and the Czech Republic. This calculation model is also customarily deployed in the analytical calculation of the pile's bearing capacity using the geotechnical software FINE Geo5. The individual calculation models presented by the authors referenced just above differ from each other in local experience, typical engineering geological conditions or piling technology. The differences between each calculation model lie in the considered mechanism of the failure of the earth environment in the vicinity of the pile, which was stated by, e.g., [5]. The analytical calculation models determining the pile's bearing capacity have been constantly developed and modified by many authors to consider different geological, geometrical, and technological aspects, see e.g., [6**?** –17]. These calculation models apply different coefficients, which can consider the geometry of the pile, the adhesion and friction in the pile body-soil interaction, the lateral earth pressure acting on the pile's shaft, and the piling technology. The analytical model given in the commentary on the STN 73 1002 standard also mentions the matter of the shortening of the pile's length in calculating the shaft friction according to Caquot-Kérisél's theory [4]. They pointed to creating an area of plastic stresses near the base of the pile, which begin to arise when the vertical load reaches the vertical bearing capacity of the pile. In the case of other frequently used calculation models, mostly in other countries, a reduction of the pile's length in calculating the shaft friction is not used in this form. The decrease of the shaft friction for the loads that reach the pile's bearing capacity and a relatively large settlement is mainly attributed to the residual stress state in the pile-body soil interface. When the effective length is applied in calculating the pile's shaft resistance, especially in the case of an embedded (end-bearing) pile, this often means that the shaft resistance of the embedded part of the pile is neglected. The aim of the study presented was to analyse the results of the instrumented static load tests of embedded piles with a focus on the distribution of axial force and the justification of a shortening of the pile's length in the calculation of its bearing capacity.

2. Calculation of the vertical resistance of the pile according to commentary on STN 73 1002

The calculation model and the detailed description of the calculation procedure are given in the commentary to the STN 73 1002 standard [4]. This calculation model is also taken by other authors, e.g., [9, 10]. The static scheme of the calculation model is shown in Figure 1. Determining the design value of the pile's vertical resistance and the influence of partial factors of different design approaches was presented by, e.g., [18]. The characteristic resistance of the pile (R_k) is given by the sum of the characteristic base resistance ($R_{b,k}$) and characteristic shaft resistance

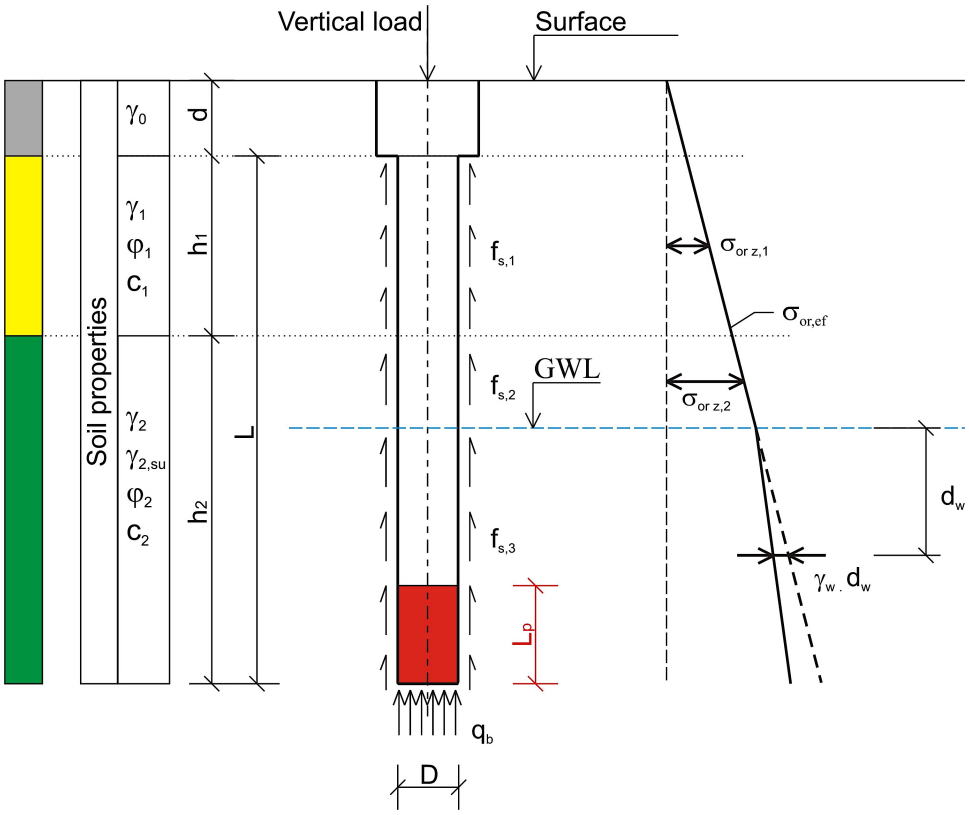

Figure 1. The static scheme of the calculation of the vertical pile resistance (according to [9]).

$(R_{s,k})$ according to the following formula:

$$R_{c,k} = R_{b,k} + R_{s,k}, \tag{1}$$

where $R_{b,k}$ can be calculated as:

$$R_{b,k} = K_1 \, A_b \, R_k, \tag{2}$$

$$R_k = c'_{d,2} \cdot N_{c,2} + q' \cdot N_{q,2} + 0.7 \cdot \gamma_2 \cdot \frac{D}{2} \cdot N_{\gamma,2}, \tag{3}$$

$$\begin{aligned} R_k =& 1.2 \cdot c'_{d,2} \cdot N_{c,2} + \left(1 + \sin \varphi'_{d,2}\right) \cdot q' \cdot N_{q,2} + \\ & 0.7 \cdot \gamma_2 \cdot \frac{D}{2} \cdot N_{\gamma,2}, \end{aligned} \tag{4}$$

where $N_{c,2}$, $N_{q,2}$, and $N_{g,2}$ are the ultimate bearing capacity factors; $\varphi'_{d,2}$ and $c'_{d,2}$ are drained shear strength properties; γ_2 is the unit weight of the soil; and q' is the effective geostatic stress in the depth of the pile's base.

The characteristic value of the shaft resistance can be determined using the following formula:

$$R_{s,k} = \pi \cdot D \sum_{i=1}^{n} h_i \cdot f_{s,i}, \tag{5}$$

where D is the diameter of the pile, h_i is the length of the pile's shaft in the i-layer, and $f_{s,i}$ is the friction on the pile's shaft in the i-layer, determined from the Equation 6 as follows:

$$f_{s,i} = K_2 \cdot \sigma_{or,i} \cdot \tan\left(\frac{\varphi'_d}{\gamma_{r,1}}\right) + \frac{c'_d}{\gamma_{r,2}}. \tag{6}$$

The values of coefficients $\gamma_{r,1}$, $\gamma_{r,2}$, and K_2 are presented by [4]. The parameter $\sigma_{or,i}$ is the geostatic stress in the middle of the i-layer.

The calculation model also states that the effective length of the pile, used in the shaft resistance calculation, can be shortened according to Caquot-Kérisel by the length of L_p (Figure 1) [4]. This reduction in length can be calculated using the following formula:

$$L_p = N_q^{2/3} \cdot \frac{D}{4}, \tag{7}$$

where N_q is the ultimate bearing capacity factor given by the formula (8) as follows:

$$N_q = \exp\left(\pi \cdot \tan \varphi'_d\right) \tan^2\left(45 + \frac{\varphi'_d}{2}\right). \tag{8}$$

Based on equations (7) and (8), the reduction length L_p is controlled by parameters D and φ'. The dependence between these input parameters and the resulting L_p value is shown in Figure 2. It can be seen that especially for coarse-grained soils, which have a value of φ'_d mostly greater than 30°, the reduction length L_p can be significant. In the case of gravel soil with an angle of shear strength of 40° and the pile with a diameter of 1.5 m, the reduction in length can reach up to 6 m.

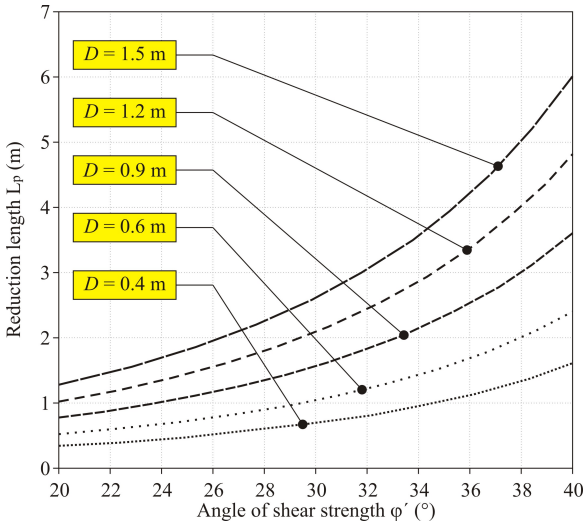

FIGURE 2. Diagram for determining L_p length.

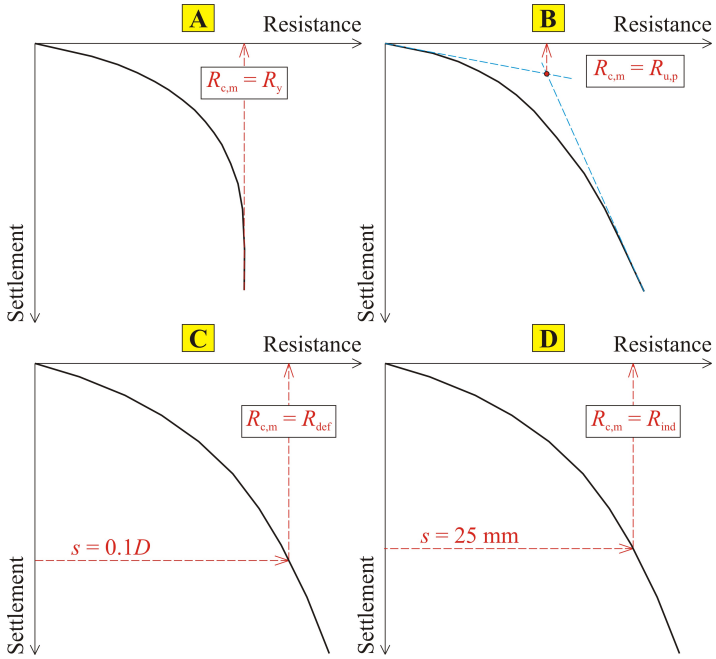

FIGURE 3. The resistance of the pile determined from a typical load-settlement curve.

3. Analysis of the results of the instrumented static load tests

A load-settlement curve of the pile can have different shapes. This mainly depends on the engineering-geological conditions and the pile's geometry. According to the shape of the load-settlement curve (Figure 3), the following resistances can be determined [9]:

- ultimate resistance (Figure 3 – A);
- resistance on the limit of the proportionality (Figure 3 – B);
- resistance on the limit of the deformation (Figure 3 – C);
- indicative resistance (Figure 3 – D).

In the case of end-bearing (embedded) piles, depending on the shape of the load-settlement curve, a settlement of the pile's head equal to 10 % of the pile diameter should be considered as the limit of the failure according to STN EN 1997-1. This corresponds with determining the characteristic resistance of the pile according to Figure 3 - C. In this case, the load-settlement curve must be executed up to the pile's settlement equal to 10 % of its diameter. The load-settlement curves of different end-bearing piles, which fulfilled the criteria of the required settlement of 10 % of the pile's diameter, were selected for the analysis presented. The tested piles were instrumented, i.e., the piles were equipped with strain gauges. This allowed for analysis of the load distribution over the pile's length.

Subsequently, the results of one tested pile are pre-

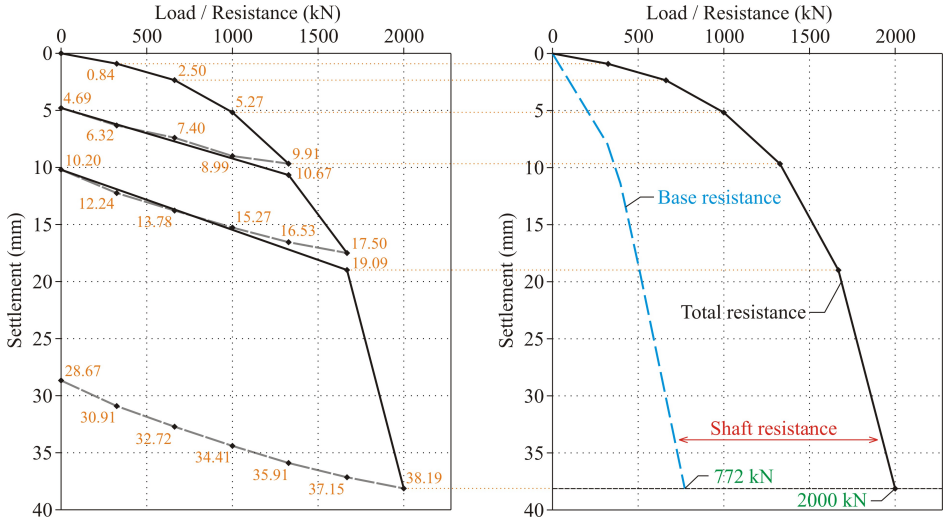

Figure 4. Load-settlement curve of the pile determined by the static load test (left), load-settlement curves of the base and total resistance of the pile used in the calculation (right).

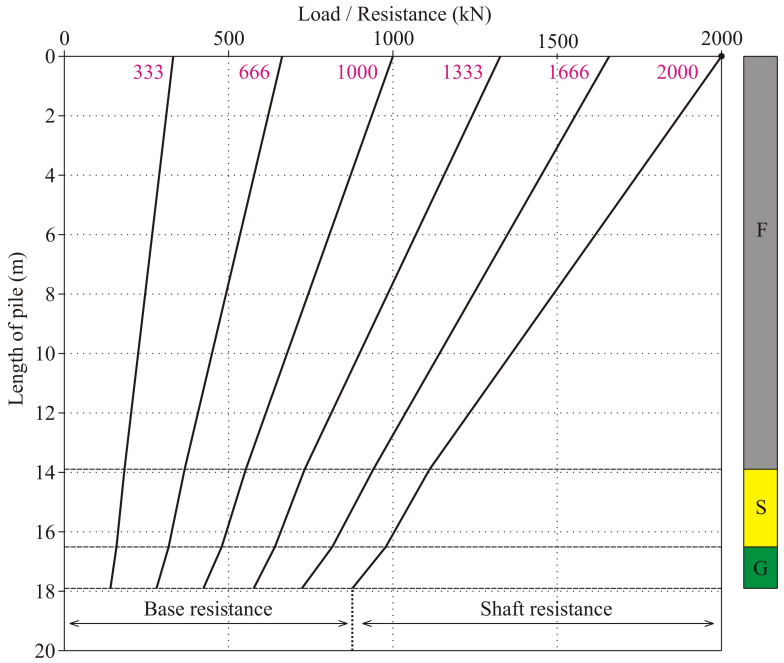

Figure 5. Load transfer over the pile's length determined by the static load test.

sented in detail. The pile tested had a diameter of 410 mm and a length of 17.9 m. The geological conditions at the testing site consisted of fine-grained soils (F) up to a depth of about 13.9 below the surface and coarse-grained soils, sand (S) and gravel (G), below them. The fine-grained soils consisted of organic soil (O) and sandy silt (MS) of soft consistency. A layer of medium-dense silty sand (SM) was located at a depth of 13.9 to 16.5 m below the surface. Gravel with fines fraction (GF) was located below the sandy soil. The tested pile was reinforced using a GEWI bar. The strain gauges were installed in couples at the depths of 0.5, 13.9, 16.5, and 17.8 m.

The load-settlement curve of the pile tested is shown in Figure 4 – left. During the test, an unloading and reloading were applied two times. After reaching the maximum loading, i.e., 2000 kN, the final unloading was also applied. The load-settlement curve of the total pile's resistance and the load-settlement curve of the pile's base resistance are shown in Figure 4 – right. When the maximum load of 2000 kN was applied, the resistance of the base reached about 772 kN. The resistance of the shaft was about 1228 kN. The load distribution over the pile's length is shown in Figure 5. The load distribution is shown for each loading step, i.e., 333, 666, 1000, 1333, 1666, and 2000 kN.

In the case of the given static load test, and similarly to the other static load tests analysed, the criterion of settlement of the pile head equal to 10 % of its diameter was met. It is evident that there was no decrease or any reduction in the shaft friction in the embedded part of the pile. The results of three static

Pile No. 1				
Vertical load [kN]	1000	1333	1666	2000
Shaft friction – Layer No. 1 – low bearing [kPa]	26	35	43	52
Shaft friction – Layers Nos. 2 and 3 – high/end bearing [kPa]	25	30	43	46
Stress below a pile's base [kPa]	3226	4376	5488	6657
Pile No. 2				
Vertical load [kN]	1000	1333	1666	2000
Shaft friction – Layer No. 1 – low bearing [kPa]	17	20	22	22
Shaft friction – Layers Nos. 2 and 3 – high/end bearing [kPa]	147	220	300	440
Stress below a pile's base [kPa]	1569	1876	2048	2256
Pile No. 3				
Vertical load [kN]	1000	1333	1666	2000
Shaft friction – Layer No. 1 – low bearing [kPa]	23	27	35	41
Shaft friction – Layers Nos. 2 and 3 – high/end bearing [kPa]	90	149	157	175
Stress below a pile's base [kPa]	1809	2003	3255	4449

Note: Layer No. 1 (O, MG, CG); Layers Nos. 2 and 3 (SM and G-F) – see Figure 5

TABLE 1. Physical properties of Holocene organic soils.

load tests of the end-bearing piles in similar geological conditions are presented in Table 1. The results present the shaft friction in layer No. 1 (fine-grained soil) – low bearing stratum, the shaft friction in layer Nos. 2–3 (coarse-grained soils) – high/end bearing stratum, and stress below the pile's base. In all the cases presented, there is no evident decrease in the shaft friction of the embedded part of the pile. On the contrary, the results clearly show that the piles take over a significant part of the shaft resistance by the friction in the embedded part of the pile – even when the pile's settlement reaches about 10 % of the pile's diameter. Tomlinson and Woodward state that a reduction in the shaft friction can only be expected when the load-settlement curve reaches the ultimate resistance of the pile (Figure 3 – A); however, in the case of the end-bearing pile this can occur for a significantly greater load when the settlement of the pile exceeded about 20 % of the pile's diameter. In the case of the static load test presented it can therefore be assumed that with the increase in the load, the ultimate resistance of the pile can be reached. In that case, a reduction in the shaft friction can be expected.

4. Parametric study on the effect of reducing the pile's length in the calculation

A simple parametric study was created to demonstrate how significant the effect of the pile's length reduction can be in the shaft resistance calculation. The geological profile consisted of two layers, i.e., low-bearing stratum (fine-grained soil) and high-bearing stratum (coarse-grained soil). The fine-grained soil was defined by the following properties: $\gamma = 20\,\mathrm{kN\,m^{-3}}$, $\varphi' = 15°$, and $c' = 10\,\mathrm{kPa}$. The coarse-grained soil was defined by the following properties: $\gamma = 20\,\mathrm{kN\,m^{-3}}$, $\varphi' = 35°$, and $c' = 0\,\mathrm{kPa}$. The total design resistance $R_{c,d}$ and the design shaft resistance $R_{s,d}$ was calculated for the end-bearing (embedded) pile of a diameter of 0.6, 0.9, 1.2, and 1.5 m; and a length of 10, 15, and 20 m. The embedded part of the pile was equal to 2 m for a 10 m long pile, 3 m for a 15 m long pile, and 4 m for a 20 m long pile. The results are presented in Table 2. The total resistance of the pile $R_{c,d}$ and the shaft resistance $R_{s,d,1}$ were calculated for the case when the reduction length was not considered. In the second case, the shaft resistance $R_{s,d,2}$ determined for the pile's length reduced by L_p, was computed. A difference $\Delta R_{s,d}$ between both shaft resistances was determined. It can be seen that considering the reduced length of the pile in the calculation can cause a significant reduction in the shaft resistance.

5. Discussion on the results presented

In general, it can be stated that the resistance of the pile and its deformation behaviour is a complex mechanism that is difficult to describe and define with a simple analytical calculation model. When the pile is continuously loaded, shaft friction is first mobilized. Subsequently, with a further increase in load, it is possible to reach the limit stress at the pile base. In the case of soils, where a significant difference occurs between the peak and critical/residual shear strength, when the pile is gradually loaded, there is a subsequent decrease in the shaft friction, as shown in Figure 6. In this case, using peak shear strength parameters in the calculation can be incorrect. This effect was not observed for the testing piles analysed. This fact is related to the decrease in the shear strength (from the peak to the residual) and is not related to neglecting the shaft friction near the base of the pile.

The shaft friction along the pile is usually not constant, e.g., [12]. Assuming homogeneous subsoil, the maximum value of the shaft friction is reached in the

	D [m]		0.6		D [m]		0.9		D [m]		1.2		D [m]		1.5	
	L_p [m]		1.552		L_p [m]		2.329		L_p [m]		3.105		L_p [m]		3.881	
L [m]	$R_{c,d}$ [kN]	$R_{s,d,1}$ [kN]	$R_{s,d,2}$ [kN]	$\Delta R_{s,d}$ [%]	$R_{c,d}$ [kN]	$R_{s,d,1}$ [kN]	$R_{s,d,2}$ [kN]	$\Delta R_{s,d}$ [%]	$R_{c,d}$ [kN]	$R_{s,d,1}$ [kN]	$R_{s,d,2}$ [kN]	$\Delta R_{s,d}$ [%]	$R_{c,d}$ [kN]	$R_{s,d,1}$ [kN]	$R_{s,d,2}$ [kN]	$\Delta R_{s,d}$ [%]
10	2370	542	354	35	4969	813	432	47	8549	1085	518	52	13140	1356	574	58
15	3849	1127	845	25	7859	1690	1056	38	13300	2254	1058	53	20190	2817	1228	56
20	5537	1920	1545	20	11060	2880	2035	29	18460	3840	2338	39	27770	4800	2453	49

Table 2. Impact of reducing the pile's length in the calculation of shaft frictions for different dimensions of the embedded piles.

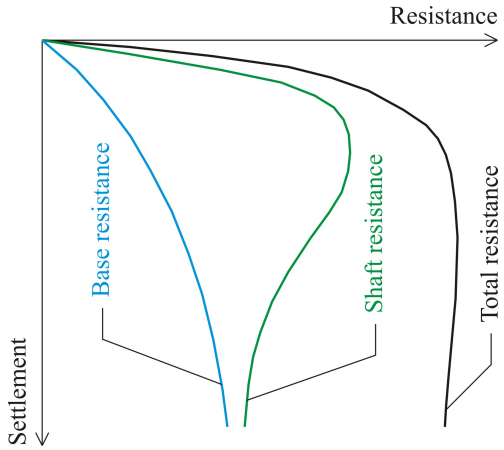

Figure 6. Load-settlement relationships – mobilization of the shaft friction and resistance at the base of the pile (according to [1]).

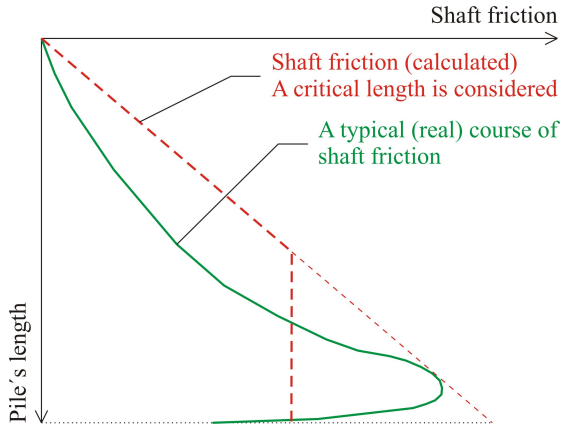

Figure 7. Transfer of the shaft friction over pile's length (according to [16]).

vicinity above the pile's base. It subsequently decreases significantly towards the pile's base (Figure 7). According to the commentary to the STN 73 1002 standard, this decrease in the shaft friction is theoretically taken into account in the calculation model precisely by introducing the effective length of the pile. However, only a decreasing in the shaft friction occurs, and therefore it is questionable if complete neglect of the shaft friction in this part of the pile is appropriate. Figure 7 also shows the calculation course of the shaft friction when applying the critical depth defined by, e.g., the NAVFAC DM7.02 standard. Under certain conditions, applying the critical depth appears to be more appropriate than neglecting the shaft friction near the pile base; however, the number of analysed static load tests did not allow a deeper analysis that could lead to a more detailed conclusion.

In the design of the pile, both the ultimate limit state (ULS) and the serviceability limit state (SLS) must be verified. The SLS condition is often stricter and thus decisive for the design of the pile. However, in the practical design of a pile foundation, a paradoxical situation often occurs when the SLS condition is fulfilled, the settlement of the piles is a relatively small value (e.g. about $20 \sim 30$ mm), but the calculated resistance of the pile does not meet the given condition. Especially in the case of end-bearing (embedded) piles, a significant resistance of the pile shaft is represented by the shaft friction of the embedded part of the pile, which is a complete neglect in the calculation when the effective length of the pile is considered. The criterion of the maximum settlement of the pile is usually lower than when the pile's settlement equals 10 % of its diameter. Then, if the SLS condition is fulfilled, it is unlikely that the pile settlement should increase to such an extent that a significant decrease in shaft friction near the pile base can be experienced. It should be noted that the analytical calculation model stated in the commentary to the STN 73 1002 standard mentions introducing the effective length of the pile into the calculation as a recommendation, not as a required condition. In the end, it is up to the designer how it will be considered in the pile design.

6. Conclusions

The analytical model for calculating the resistance of a single pile, given in the commentary to the STN 73 1002 standard, introduces the recommendation of applying the pile's effective length into the pile's shaft resistance calculation, according to the Caquot-Kérisel theory. Theoretically, the formation of an onion-shaped area of plastic stresses near the pile base is assumed when the load approaches the ultimate resistance of the pile. As a result of this effect,

the shaft friction near the pile base should be ignored. Especially in the case of end-bearing (embedded) piles, this may mean that the resistance of the embedded part of the pile is not included in the total resistance of the pile, although its contribution to the pile's total resistance can be significant. The results of the instrumented static load tests were analysed, in which the settlement of the pile head equal to 10 % of their diameter was achieved, and it was assumed that the resistance on the limit deformation (Figure 3 – C) was reached. The results of the static load tests showed that even when the pile head settled at 10 % of its diameter, there was no reduction in the shaft friction in the embedded part of the pile; on the contrary, significant shaft friction was also recorded in the embedded part of the pile. Based on the theoretical review, it can be assumed that a decrease in shaft friction could only be noted when the ultimate resistance of the pile is reached, which is particularly difficult for end-bearing (embedded) piles of the given geometry installed in similar geological conditions. The application of the effective (reduced) or actual length of the pile in the calculation of the resistance is at the discretion of the designer/statics. In the case of end-bearing (embedded) piles, where the serviceability limit state condition is fulfilled, the pile deformation does not exceed 10 % of its diameter – it seems more appropriate to consider the total length of the pile in the calculation of the resistance.

References

[1] M. Tomlinson, J. Woodward. *Pile design and construction practice*. Taylor & Francis e-Library, 5th edn. p. 551, 2007.

[2] D. A. Brown, S. Dapp, W. R. Thompson, et al. Geotechnical engineering circular no. 8 – Design and construction of continuous flight auger (CFA) piles p. 294, 2007.

[3] K. Fleming, A. Weltman, M. Randolph, K. Elson. *Piling engineering*. Taylor & Francis e-Library, 3rd edn. p. 398, 2008.

[4] R. Pochman, J. Šimek. Pile foundations [in Czech – Pilotové základy]. Commentary to ČSN 73 1002, 1.vyd. Praha, Vydavatelství norem. 1989. p. 75. ISBN 80-85111-04-7.

[5] C. Viggiani, A. Mandolini, G. Russo, et al. *Piles and pile foundations*. Taylor & Francis, London, UK. p. 278, 2012.

[6] S. Škrabl. Bearing capacity and settlement of vertically-loaded piles. In *Deep Foundations 2002: An International Perspective on Theory, Design, Construction, and Performance*, pp. 53–63. 2002. https://doi.org/10.1061/40601(256)5

[7] J. Zhang, L. Hanlong, G. Yang. A simplified method for calculating ultimate bearing capacity of cast-in-place concrete pipe pile with large diameter in sandy soil. In *Advances in Pile Foundations, Geosynthetics, Geoinvestigations, and Foundation Failure Analysis and Repairs*, pp. 75–81. 2011. https://doi.org/10.1061/47631(410)9

[8] J. Mecsi. Geotechnical engineering examples and solutions using the cavity expanding theory Hungarian Geotechnical Society, 2013, p. 232.

[9] J. Masopust. *Bored piles* [in Czech – Vrtané piloty]. Prague, Čenek a Ježek s.r.o., 1994, p. 263.

[10] J. Hulla, P. Turček. *Foundation engineering* [in Slovak – Zakladanie stavieb]. Jaga Group s.r.o., Bratislava, 1998, p. 310.

[11] M. Randolph, R. Dolwin, R. Beck. Design of driven piles in sand. *Geotechnique* **44**(3):427–448, 1994. https://doi.org/10.1680/geot.1994.44.3.427

[12] B. Wrana. Pile load capacity–calculation methods. *Studia Geotechnica et Mechanica* **37**(4):83–93, 2015. https://doi.org/10.1515/sgem-2015-0048

[13] J. Mihalik, F. Gago, M. Bukova. Determination of experimental bearing capacity piles. In *Juniorstav 2022: Proceedings of the 24th International Conference of Doctoral Students*. Brno: ECON publishing, pp. 297–302, 2022.

[14] M. Drusa, J. Vlcek, F. Gago, et al. *Modern methods of designing geotechnical structures*. Žilina: University of Zilina, 2019, p. 277.

[15] M. Drusa, F. Gago, J. Vlček. Contribution to estimating bearing capacity of pile in clayey soils. *Civil and Environmental Engineering* **12**(2):128–136, 2016. https://doi.org/10.1515/cee-2016-0018

[16] M. F. Randolph, J. P. Carter, C. P. Wroth. Driven piles in clay—the effects of installation and subsequent consolidation. *Géotechnique* **29**(4):361–393, 1979. https://doi.org/10.1680/geot.1979.29.4.361

[17] J. Mihálik, F. Gago, J. Vlček, M. Drusa. Evaluation of methods based on CPTu testing for prediction of the bearing capacity of CFA piles. *Applied Sciences* **13**(5):2931, 2023. https://doi.org/10.3390/app13052931

[18] J. Stacho. Calculation design of bored piles. In *Juniorstav 2022: Proceedings of the 14th International Conference of Doctoral Students*, Brno: VUT, 2012.